Journal of Ocean, Mechanical and Aerospace
-Science and Engineering-, Vol.16

February 20, 2015

A New Implementation of Vortex Lattice Method Applied to the Hydrodynamic Performance of the Propeller-Rudder

Hassan Ghassemi,[a,*] and Farzam Allafchi, [a]

[a)]*Department of Ocean Engineering, Amirkabir University of Technology (AUT), Iran*

*Corresponding author: gasemi@aut.ac.ir

Paper History

Received: 2-February-2015
Received in revised form: 7-February-2015
Accepted: 17-February-2015

ABSTRACT

This paper describes a new implementation of a vortex lattice method based on modified lifting line (VLML) for ship propeller-rudder. Method has been employed to estimate hydrodynamic performance and flow fields, for design and analysis. For this purpose, the results obtained using theoretical model are validated against experimental data, carried by Tamashima et al. [18], concerning to propulsor system. Comparison of these results indicates good agreement with those of the experimental data. Therefore the method can be used as a fast tool for preliminary design and analysis.

KEY WORDS: *Vortex Lattice Method; Hydrodynamic Performance; Propeller-Rudder.*

NOMENCLATURE

Γ	Vortex Strength
$\vec{s}$	Unit Vector Tangent to Vortex
$\vec{r}$	Distance Vector
dl	Differential Element of Length along the Vortex Line
F_a	Axial Force
F_t	Tangential Force
u_a^*	Axial Induced Velocity
u_t^*	Tangential Induced Velocity
ω	Rotational Velocity of Propellers
r	Radius of Blade's Element
φ	Blade Pitch Angle
β_{in}	Hydrodynamic Pitch Angle
β_ω	Pitch Angle of The Helical In The Wake
r_c	Control Point Radius
r_v	Vortex Point Radius
C_L	Lift Coefficient
T	Thrust
Q	Torque
Z	Number of Blades
J	Advanced Coefficient
K_T	Thrust Coefficient
K_Q	Torque Coefficient
η	Efficiency

1.0 INTRODUCTION

Propellers work as the whole or the main part of the propulsion systems of marine vehicles, thus the prediction and the calculation of the propulsor performance is a momentous matter for hydrodynamic specialist and designers; because, these calculations and predictions play important roles in achieving the favorable design speed of vessels with the lowest consumption of energy.

For this purpose, considerably improvements have been fulfilled during the past decades, thus, several methods are available based on different levels of sophistication, each of them have their own benefits and disadvantages. The most precise methods are three-dimensional viscous flow models, which the three-dimensional Reynold-Average Navier-Stockes (RANS) equations have been solved iteratively. Following are the advanced lifting surface methods which solve RANS equations to account viscous effects near the solid walls [1]. The next methods are the boundary element method (BEM) which generates

elements just at the boundary of body which leads to the reduction of computing time and cost [2]. Other innovative procedures were presented which tend to reduce the cost of calculations. Momentum and blade element theory were combined to predict the performance of marine propellers compared results with those found using RANS equation, comparison indicates that simple theories are applicable as well as more complicated one [3].

The conventional vortex lattice method (VLM) is a subclass of the lifting surface method which replaces the continuous distribution of vortices by a set of concentrated line elements of constant strength [4]. This method was optimized by Olsen (2001) and was used by Kinnas and Coney (1988) and Coney (1989) for the modeling of ducted propellers [5,6,7]. Moreover, Performance analysis of podded propulsors has been made with a vortex lattice method [8].

Lifting line is another method which utilizes concentrated vortices to predict lifting body performances. Lifting line is known as a fast procedure with simple formulation, which is used for hydrofoils mainly [9,10]. This method is being used as a powerful method for studying hydrodynamic behavior near free surface [11,12].

A combination of VLM and lifting line was presented, which uses VLM concepts with the simplicity of the lifting line [13]. This method has been used for off design condition and ducted propellers separately, they showed good result from this method [14,15]. Driss et al. (2012) investigated the effect of multiple Rushton impellers configurations on hydrodynamics and mixing performance in a stirred tank by CFD code [16]. Recently, Rui and Koto (2014) carried out prediction of propeller performance using quasi-continuous method [17].

The main tasks involved in this method include the panel generation, calculation of the induced velocities per unit-strength vortices and the obtaining and solving the equations, to calculate total thrust, torque and efficiency. In this paper, the hydrodynamic analysis of some conventional propellers and a propeller-rudder are performed using VLML. Then the results are compared with experimental data of other works done.

2.0 MATHEMATICAL FORMULATION

Considering a three-dimensional vortex of constant strength (Γ), acting along the entire length of the line describing its path through space, the induced velocities are calculated using Biot-Savart's law

$$\vec{V} = \frac{\Gamma}{4\pi}\oint \frac{\vec{s}\times\vec{r}}{|r|^3} dl \qquad (1)$$

An element of blade is shown in Figure 1. which V_A and V_T are the axial and tangential velocities of input flow, V^* is the total velocity and finally F_i, F_v and F are the induced, frictional and total force acting on the element, respectively.

Using Kutta-Joukowski's theorem induced force can be obtained and by suitable resolution of forces, the axial and tangential forces are fulfilled.

$$F_i = \rho V^* \Gamma$$

$$F_a = [F_i cos\beta_{in} - F_v sin\beta_{in}]$$

$$F_t = [F_i sin\beta_{in} + F_v cos\beta_{in}] \qquad (2)$$

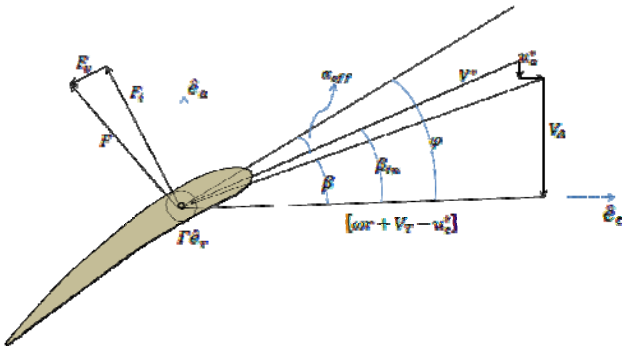

Figure 1: Velocity triangles and forces on a blade element.

2.1 Vortex Lattice Implementation

The lattice is structured in two main zones, i.e. blade zone and wake region. Blade zone is modeled by bound vortices that are expanded between two vortex points with constant strength and radial direction. Wake is made up of some twin semi-infinite helical vortices (trailing vortex) with opposite directions, which are situated in bound vortices ends (vortex points). Fig. 2 shows the lattice explained. The force analysis is performed at control points which are determined with cosine spaced.

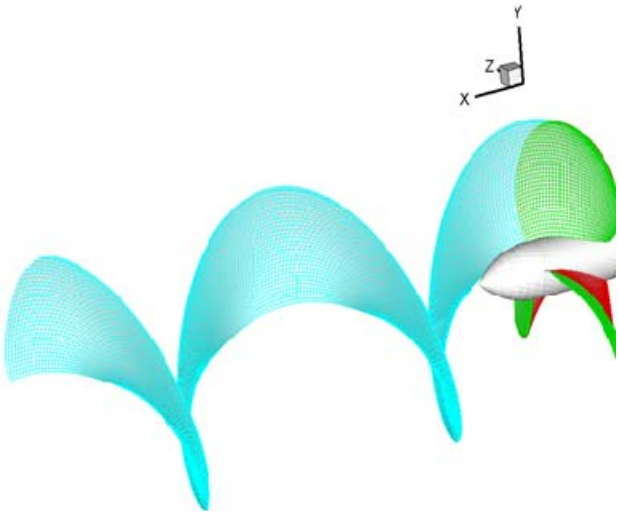

Figure 2: Vortex lattice modeling

2.2 Calculation of Induced Velocities

The induced velocities are computed at control points, each horseshoe vortex induces a velocity at every control point, and thus the total induced velocity at control points is computed as follows:

$$u_a^*(n) = \sum_{i=1}^{N} \Gamma_i \, \bar{u}_a^*(n,i)$$
$$u_t^*(n) = \sum_{i=1}^{N} \Gamma_i \, \bar{u}_t^*(n,i) \quad (3)$$

where $\bar{u}_a^*(n,i)$ and $\bar{u}_t^*(n,i)$ are the axial and tangential velocity induced at the n'th control point by a unit-strength horseshoe vortex surrounding panel. Whereas the control points are located at the bound vortex's axis, they do not induce velocity at control points, therefore the induced velocity at control points are just due to trailing vortices as follows:

$$u_a^*(n,i) = \bar{u}_a(n,i) - \bar{u}_a(n,i+1)$$
$$u_t^*(n,i) = \bar{u}_t(n,i) - \bar{u}_t(n,i+1) \quad (4)$$

where $\bar{u}_a(n,i)$ and $\bar{u}_t(n,i)$ are velocity induced by a single unit-strength trailing vortex of the i'th panel at the n'th control point, which are computed using the approximation by Wrench for a constant-pitch helical vortex filament as follows:
for $r_c(n) < r_v(i)$:

$$\begin{cases} \bar{u}_a(n,i) = \frac{Z}{4\pi r_c}(y - 2Zyy_0F_1) \\ \bar{u}_t(n,i) = \frac{Z^2}{2\pi r_c}(y_0F_1) \end{cases} \quad , \quad (i,n = 1,2,\dots,N)$$

and for $r_c(n) > r_v(i)$:

$$\begin{cases} \bar{u}_a(n,i) = -\frac{Z^2}{2\pi r_c}(yy_0F_2) \\ \bar{u}_t(n,i) = \frac{Z}{4\pi r_c}(1 + 2Zy_0F_2) \end{cases} \quad (5)$$

where

$$F_1 = \frac{-1}{2Zy_0}\left(\frac{1+y_0^2}{1+y^2}\right)^{0.25}\left\{\frac{1}{U^{-1}-1} + \frac{1}{24Z}\left[\frac{9y_0^2+2}{(1+y_0^2)^{1.5}} + \frac{3y^2-2}{(1+y^2)^{1.5}}\right] ln\left(1 + \frac{1}{U^{-1}-1}\right)\right\} \quad (6)$$

$$F_2 = \frac{-1}{2Zy_0}\left(\frac{1+y_0^2}{1+y^2}\right)^{0.25}\left\{\frac{1}{U-1} - \frac{1}{24Z}\left[\frac{9y_0^2+2}{(1+y_0^2)^{1.5}} + \frac{3y^2-2}{(1+y^2)^{1.5}}\right] ln\left(1 + \frac{1}{U-1}\right)\right\} \quad (7)$$

$$U = \left(\frac{y_0\left(\sqrt{1+y^2}-1\right)}{y\left(\sqrt{1+y_0^2}-1\right)} e^{\left(\sqrt{1+y^2}-\sqrt{1+y_0^2}\right)}\right) \quad (8)$$

$$y_0 = \frac{1}{tan\beta_\omega}$$
$$y = \frac{r_c}{r_v tan\beta_\omega} \quad (9)$$

where β_ω is the pitch angle of the helical in the wake for the vortex points as computed below

$$tan\beta_\omega = \left(1.5 - \left({}^{P}/_{D}\right)\right) tan\varphi + \left(\left({}^{P}/_{D}\right) - 0.5\right) tan\beta \quad (10)$$

where ${}^{P}/_{D}$ is the ratio of the pitch to propeller diameter, this equation is fulfilled through several trail and errors.

2.3 Governing Equations

Based on Prandtl's thin airfoil theory:

$$C_L(i) = \frac{2\Gamma_i}{V_{(i)}^* \, c(i)} = 2\pi\alpha_{eff}(i) \quad (11)$$

where i indicates the quantities at the i'th panel and c is the chord

$$\alpha_{eff}(i) = \varphi(i) - \beta_{in}(i) \quad (12)$$

The following angles can be computed using geometrical equations. Replacing the values from the last equations, a nonlinear simultaneous equation is obtained with N unknown $(\Gamma_1, \Gamma_2, \dots, \Gamma_N)$, that should be solved iteratively. In the present study, Newton's method for systems has been employed to solve the mentioned equation. This procedure converges rapidly however, in some cases it may be difficult to choose an appropriate initial guess. Therefore, steepest descent method (SDM) was employed to improve it.

2.4 Propeller Formulation

Solving the simultaneous equation results to the circulation distribution, which eventuate to the hydrodynamic forces. Fig. 3 shows circulation distribution computed by code for a propeller in different operating conditions. The total thrust and torque of the propeller is obtained from integrating the elements of axial force and torque over the radius.

$$T = Z\int_{r_h}^{R} F_a dr\,, \qquad Q = Z\int_{r_h}^{R} rF_t dr \quad (13)$$

The hydrodynamic coefficients of the propeller are determined as

follows:

$$J = \frac{V_A}{nD} \qquad K_T = \frac{T}{\rho n^2 D^4}$$

$$K_Q = \frac{Q}{\rho n^2 D^5} \qquad \eta = \frac{J}{2\pi}\frac{K_T}{K_Q} \tag{14}$$

where n is the rotational speed.

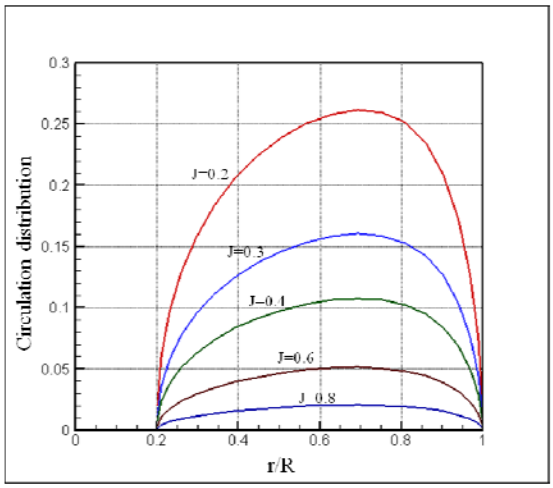

Figure 3: Circulation distribution for B4,70, P/D = 1.0, ($GAMMA = \frac{\Gamma}{2\pi R V_s}$).

2.5 Rudder Formulation

Rudder can be considered as a simplified propeller blade, which is placed in the wake of propeller therefore propeller induce different velocity at every rudder panel. For considering the effect of propeller blades and wake, the inflow velocity at each rudder panel is calculated using super-position. Different terms of rudder inflow are classified below:

- Axial inflow velocity of propeller, V_A.
- Tangential inflow velocity of propeller, V_T.
- Induced velocity due to helical vortices (propeller wake).
- Induced velocity due to bound vortices (propeller blades).
- Rudder's trailing vortices induced velocity.

3.0 PROPELLER'S NUMERICAL MODELING

In this study, to determine the open-water characteristics of the propeller, different types of propeller models has been performed by means of VLML. Undisturbed velocity (V_A) was considered as a variable parameter in order to obtain different values of advanced coefficient (J) while the rotational speed is fixed. To achieve the panel independency of the model, several models were created with different panel size. The panels' size is reduced step wisely until the results converged to a same point after a specific step. Fig. 4 shows computed hydrodynamic parameters versus number of panels. The propeller blade has been divided into thirty panels on both radial and chordwise directions. Therefore, all panels are for the propeller is about 2700 panels.

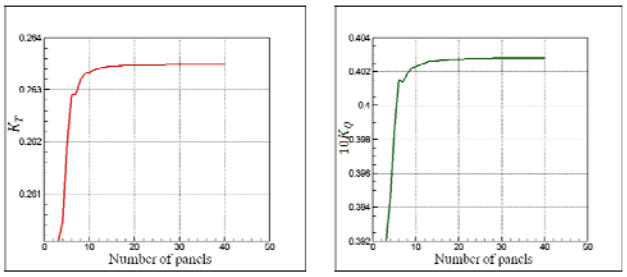

Figure 4: Hydrodynamic performances versus number of panels on both radial and chordwise directions

Comparison between VLML results and experimental data is given in Fig. 5. As a general indication, the accuracy in the prediction of propeller performance using VLML is acceptable, which depends on the value of J and P/D. In particular, the best results are fulfilled when J is rather close to propeller design point (maximum efficiency). In the mentioned region the maximum discrepancy from experimental results being in order of 5% in prediction of K_T , K_Q and η.

Results for P/D=0.5 are not as accurate as the other ones found for other pitch ratios. Increasing pitch ratio in minimum J region causes an increase in discrepancy between calculated torque coefficient and experimental data. For P/D=0.5, the thrust is overestimated near minimum J, this trend became inversed by increasing pitch ratio. This is due to the difference in operating condition of propellers. For a propeller with high pitch ratio operating at minimum J in super heavy condition, the 3D effects are significant, but in this specific work were neglected.

The wake is modeled with elaborate helical vortex filaments, which are constant-pitch and constant-radius. In a real case, the wake angle and pitch are as the function of several parameters such as advanced coefficient (J), which is neglected. These assumptions are for simplicity, but cause an error in the performance prediction of a propeller in off-design condition.

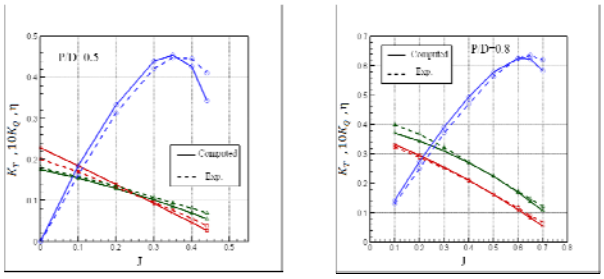

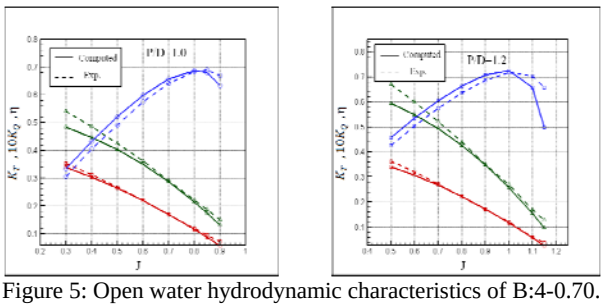

Figure 5: Open water hydrodynamic characteristics of B:4-0.70.

The most prominent task in this procedure is prediction of the wake angle, which used to be calculated iteratively. In this method, this angle is related to pitch ratio without iteration, which causes precipitation of the calculations, as it can be run in a conventional personal computer in a few seconds.

4.0 PROPELLER-RUDDER'SNUMERICAL MODELING

VLM was applied to predict hydrodynamic performances of rudder as a part of propulsion system. Rudders work in propeller wake, thus effects of propeller play important role in rudder performance. These effects are considered as induced velocity behind the propeller. Figure 6 shows induced velocity components in different positions, where *X* is the distance behind the propeller. The computed results are validated against experimental data carried out by Tamashima et al. (1993), which acceptable agreement was observed [18]. Discrepancies are not enough acceptable at low radius ratios; this is owing to neglecting the hub effects, whereas at higher radius predictions are admissible. The main dimension of the propeller-rudder (employed by Tamashima et al.) is presented in Tables 1 and 2.

The axial induced velocity component shows more accurate predictions rather than tangential velocity, particularly in maximum values. The error is due largely to simplifying assumption of helical trailing vortex such as constant-pitch and constant-radius. The axial component is the most important one for rudder analysis. Fig. 7 shows the contour of axial velocity at four distances behind the MP101 propeller. Tangential component of induced velocity causes forces on two region of rudder (up and down), which neutralize each other due to axis-symmetrical attributes of propeller's wake. Thus the obtained result of force analysis of rudder in presence of propeller would be reliable, (Fig. 8). The results show good agreement in all operating conditions except the rudder angles higher than 30[deg.] and for high advance coefficient (J =0.55), which is attributed to cavitation, that is neglected in present method.

Table 1: Dimension of propeller models

Propeller type	MP24	MP101
Diameter [mm]	210	220
Exp. Area Ratio	0.62	0.55
Pitch Ratio	0.89	0.80
Boss Ratio	0.1888	0.18
No. of Blades	5	4
Rake Angle [deg.]	-12.03	10.0
Thickness Ratio	0.0405	0.050
Blade Section	MAU	MAU

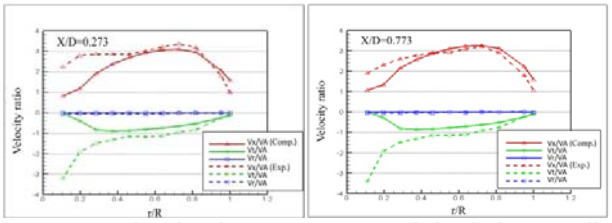

Figure 6: Induced velocity components behind the propeller without rudder (MP24, J=0.3)

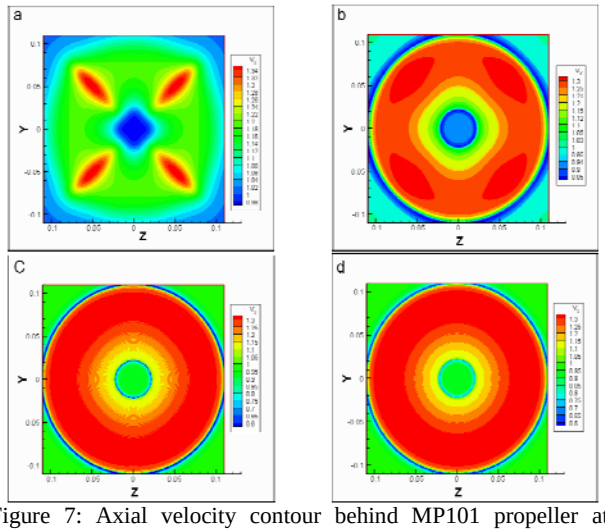

Figure 7: Axial velocity contour behind MP101 propeller at J=0.6; a) X/D=0.05 b) X/D=0.15 c) X/D=0.25 d) X/D=0.35

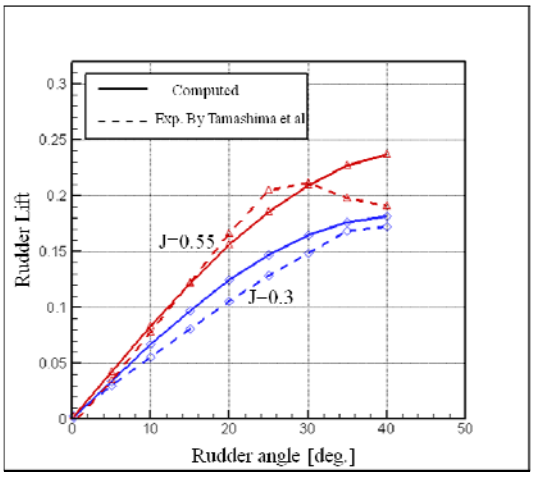

Figure 8: Rudder Lift at different operating conditions in presence of propeller (MP101-MR21)

Table 2: Dimensions of rudder models

Rudder Type	MR21
Shape	REC
Span[mm]	240
Chord [mm]	160
Type of Section	NACA 0015

The total thrust and torque of propeller-rudder system calculated using present method. An increase in rudder angle causes increase in rudder drag, thus the whole propulsion thrust decreases, as seen in Fig. 9. In the present calculations, propeller-rudder is discretized by 2700 panels for the propeller and 600 panels for the rudder, totally is about 3300 panels.

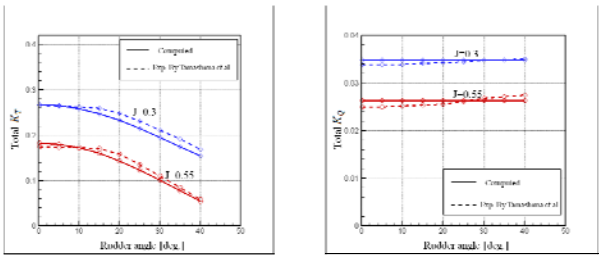

Figure 9: Total thrust and torque of the whole propulsion system at different operating conditions (MP101-MR21).

6.0 CONCLUSIONS

In conclusion, a new implementation of the VLML based on lifting line was presented, which estimates the wake angle as a function of pitch ratio. The prepared code analyzes propellers without iteration, which causes reduction in numerical cost and time.

In the case study, four types of different propellers, and one propeller along with rudder as a whole propulsion system were analyzed to predict hydrodynamic performance using the mentioned code. The results were validated against experimental data. The following results can be extracted from the comparisons:

- The performance predictions are admissible especially at and before design point (the appropriate region for designers) for propellers.
- Present method can be used as a fast method for preliminary propeller and propeller-rudder design and analysis, because it is inexpensive to run.
- In the performance prediction of propellers, the results for minimum *J* and which is higher than design point are not acceptable.
- The source of the above errors within VLML is attributed to the poor prediction of the wake angle and neglecting 3D effects in this method, which is intrinsically two-dimensional.

REFERENCES

1. Black, S.D. (1997).*Integrated lifting-surface/Navier–Stokes design and analysis methods for marine propulsors*, Ph.D. Thesis Massachusetts Institute of Technology.
2. Ghassemi, H., Ghadimi, P. (2011).*Numerical Analysis of the high skew propeller of an underwater vehicle*, J. Marine Science & Application 10(3), 289-299.
3. Benini, E. (2004).*Significance of blade element theory in performance prediction of marine propellers*, Ocean Engineering 31, 957-974.
4. Carlton, J. (2007).*Marine propellers and propulsion*, second edition, Butterworth-Heinemann Ltd, London.
5. Olsen, A. S. (2001).*Optimization of propellers using the Vortex-Lattice Method*, Ph. D. Thesis Technical University of Denmark.
6. Kinnas, S. A., Coney, W. B. (1988).On the optimum ducted propeller loading, *In proc. propellers '88 symposium*, Jersey city 1.1-13, N. J: SNAME.
7. Coney, W. B. (1989).*A method for the design of a class of optimum marine propulsors*, Ph.D. Thesis Massachusetts Institute of Technology.
8. Bal, S., Guner, M. (2009).*Performance analysis of podded propulsors*, Ocean Engineering, 36, 556-563.
9. Breslin, J. P., Andersen, P. (1994).*Hydrodynamics of marine propellers*, University press, Cambridge UK.
10. Molland, A. F., Turnock, S. R. (2007).*Marine rudder and control surfaces*, Butterworth-Heinemann Ltd, London.
11. Liang, H. and Zong Z. (2011).*A Lifting Line Theory for a Three-dimensional Hydrofoil*, J. Marine Science & Applications, 10, 199-205.
12. Zong, Z., Liang, H., Zhou L. (2012).*Lifting line theory for wing-in-ground effect in proximity to a free surface*, J. Engineering Mathematic, 74, 143-158.
13. Kerwin, J.E., Coney, W.B. & Hsin, C.-Y. (1986).Optimum circulation distributions for single and muIti-component propulsors. *In Proc. of 21st ATTC*, ed. R.F. Messalle, 53-92. Washington, D.C.: National Academy Press.
14. Flood, K. M. (2009).*Propeller performance analysis using lifting line theory*, M.S. Thesis, Massachusetts Institute of Technology.
15. Stubblefield, J.M. (2008).*Numerically-Based ducted propeller design using vortex lattice lifting line theory*, M.S. Thesis, Massachusetts Institute of Technology.
16. Driss, Z., Karray, S., Chtourou, W. , Kchaou, H., Salah Abid M. (2012).*A Study of Mixing Structure in Stirred Tanks Equipped With Multiple Four-Blade Rushton Impellers*, The Achieves of Mechanical Eng., Vol. LIX, No. 1.
17. Hao Rui, Jaswar Koto, (2014).*Prediction of Propeller Performance Using Quasi-Continuous Method*, Journal of Ocean, Mechanical and Aerospace-Science and Engineering, Vol.10 August 20.
18. Tamashima, M., Matsui, K., and Yamazaki, R. (1993).The method for predicting the performance of propeller-rudder system with rudder angle and its application to the rudder design. *Transactions of the West-Japan Society of Naval Architects. 86, (in Japanese).*